Nuclear Engineering and Technology 54 (2022) 4679–4683

Contents lists available at ScienceDirect

Nuclear Engineering and Technology

journal homepage: www.elsevier.com/locate/net

Original Article

Development of a diverging collimator for environmental radiation monitoring in the industrial fields

Dong-Hee Han [a], Seung-Jae Lee [b], Jang-Oh Kim [c], Da-Eun Kwon [a], Hak-Jae Lee [d], Cheol-Ha Baek [a, e, *]

[a] Department of Medical Health Science, Kangwon National University, Samcheok, 25949, South Korea
[b] Department of Radiological Science, Dongseo University, Busan, 47011, South Korea
[c] Health and Medical Education Research Institute, Kangwon National University, Samcheok, 25949, South Korea
[d] ARALE Laboratory Co., Ltd., Seoul, 02843, South Korea
[e] Department of Radiological Science, Kangwon National University, Samcheok, 25949, South Korea

ARTICLE INFO

Article history:
Received 29 June 2022
Received in revised form
7 August 2022
Accepted 8 August 2022
Available online 12 August 2022

Keywords:
Industrial fields
Radiation monitoring
Diverging collimator
Monte Carlo simulation
Location of sources

ABSTRACT

Environmental radiation monitoring is required to protect from the effects of radiation in industrial fields such as nuclear power plant (NPP) monitoring, and various gamma camera systems are being developed. The purpose of this study is to optimize parameters of a diverging collimator composed of pure tungsten for compactness and lightness through Monte Carlo simulation. We conducted the performance evaluation based on spatial resolution and signal-to-noise ratio for point source and obtained gamma images and profiles. As a result, optimization was determined at a collimator height of 60.0 mm, a hole size of 1.5 mm, and a septal thickness of 1.0 mm. Also, the full-width-at-half-maximum was 3.5 mm and the signal-to-noise ratio was 53.5. This study proposes a compact 45° diverging collimator structure that can quickly and accurately identify the location of the source for radiation monitoring.

1. Introduction

According to a database on Nuclear Power Plants (NPPs) by the International Atomic Energy Agency (IAEA), as of May 2022, there are 200 NPPs that have been permanently shut down worldwide, of which 21 had been decommissioned by 2021 [1]. Also, more than half of the NPPs in operation have been operating for more than 30 years, so the decommission industry is drawing attention as they age. Radiation monitoring is essential for preventing radiation exposure and contamination from radioisotopes and for systematic management of radioactive waste generated during the decontamination and decommissioning processes [2,3].

It is also reported that radioactive gases and liquids are released to the outside during normal operation, and it is important to verify compliance with permitted emission limits and other regulatory requirements for each element [4]. The beta/gamma emitters to be considered are ^{137}Cs, ^{134}Cs, ^{144}Ce, ^{106}Ru, and ^{125}Sb, and efforts are underway to minimize the effects of radioactivity on the environment. In particular, the U.S. Nuclear Regulatory Commission (NRC) has regularly conducted environmental radiation monitoring to analyze samples, at which time ^{137}Cs are evaluated as a major contributing factor [5].

Environmental radiation monitoring is a system that detects gamma rays and images them in real time. Gamma cameras equipped with collimators have been used to identify the location of sources [6,7]. Collimators play an important role in detecting and locating source points in the monitoring of industrial fields as well as medical fields. In addition, with the recent compactness of equipment and the development of unmanned equipment such as drones and robots, innovative methods are being sought to prevent exposure to workers and to control equipment remotely. Likewise, gamma cameras must be compact [8,9].

A pinhole collimator, which has been used to secure a wide area, is produced through a casting type manufacturing method. But, since gamma rays are selectively collected through one hole to form an image, there is a disadvantage of low sensitivity. This limits rapid source identification and operating time, as well as causing a drastic decrease in sensitivity in the edge area at a solid angle [10,11].

* Corresponding author. Department of Medical Health Science, Kangwon National University, Samcheok, 25949, South Korea.
E-mail address: baekch@kangwon.ac.kr (C.-H. Baek).

https://doi.org/10.1016/j.net.2022.08.004

Recently, the Direct Metal Laser Sintering (DMLS) 3D printing method that melts metal powder has been introduced, making it possible to manufacture physically complex structures that have limitations in casting type. The diverging collimator had been proposed as an alternative to solve the problem of performance degradation in the edge area within the pinhole collimator's field-of-view (FOV) and ensure excellent spatial resolution at the same time and is drawing attention [12,13].

In this study, the parameters of the diverging collimator that can be mounted within a compact gamma camera were optimized using the Monte Carlo simulation tool Geant4 Application for Emission Tomography (GATE) v9.0. Gamma images and the Point Spread Function (PSF) for ^{137}Cs were obtained using a collimator, and sensitivity, spatial resolution, and Signal-to-Noise Ratio (SNR) were independently calculated.

2. Methods and materials

The performance parameters of the diverging collimator are collimator height, hole size, and septal thickness, and the higher is the collimator height, the lower is the absorption rate of gamma rays reaching the detector. Therefore, the sensitivity decreases; this tends to be the same when the size of each hole decreases and the septal thickness increases. Theoretically, R_{divg} (collimator resolution) and ρ (efficiency) can be calculated using the following formulas and the elements in Fig. 1 [14].

$$R_{divg}(b,l) = \left[d\left(l_{eff}+b\right) \Big/ l_{eff}\right][1/cos\theta]\left[1+\left(l_{eff} \Big/ 2f\right)\right]$$

$$\rho_{divg}(b,l) \approx K^2\left(d \Big/ l_{eff}\right)^2\left[d^2 \Big/ (d+t)^2\right][(\mathrm{f}+\mathrm{l}) / (\mathrm{f}+\mathrm{l}+\mathrm{b})]$$

Where b is the distance from a point source to the surface of the collimator, l is the collimator height, and l_{eff} is the effective height of the collimator, which is derived by $l_{eff} = l - 2/\mu$ through the mass attenuation coefficient (μ_m), density, and linear attenuation coefficient (μ) of the collimator's material. The variable d is the hole size on the bottom, t is the septal thickness, and θ is the source angle. The variable f is the focal length, and in this study, the diverging collimator fixed the FOV to 45°. Various studies have reported that these factors have mainly affected performance, and a comparative analysis with theoretical calculations has been conducted [12,15].

In general, pinhole and diverging collimator types have been used to detect a wide FOV with a small size. The materials of the proposed collimator to counter gamma rays of high energy are tungsten, lead, gold, and depleted uranium, with high atomic number, density, and superior photon-stopping power [16,17]. In this study, a diverging collimator of pure tungsten (Atomic number: 74, Atomic weight: 183.8 u, and density: 19.3 g/cm^3) was selected as applicable to metal 3D printing technology that has recently been in the spotlight and can compensate for the shortcomings of pinhole collimators.

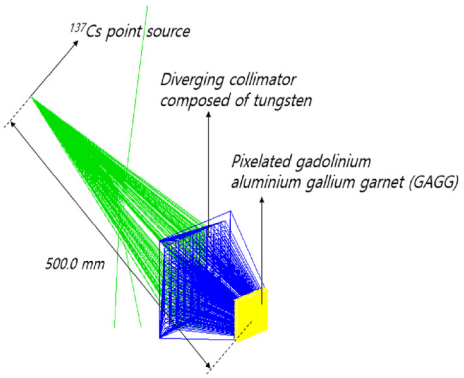

Fig. 2. Geometry in geant4 application for tomographic emission (GATE) using point sources.

The detection system used a gadolinium aluminum gallium garnet, $Gd_3Al_2Ga_3O_{12}$ (GAGG). GAGG has a density of 6.6 g/cm^3, is non-hygroscopic, and emits about 57,000 photons per MeV, which is excellent in performance. Also, it has a relatively short decay time of 90 ns or less. The overall dimension is 25.4 × 25.4 × 3.5 mm^3, and pixels of 0.5 × 0.5 × 3.5 mm^3 were arranged and divided by 42 × 42 to obtain a high-resolution image that could locate the source [18].

The radioactive source was set to ^{137}Cs (γ: 662.0 keV) and was located 500.0 mm from the detector surface. The overall structure is shown in Fig. 2. At this time, the energy window was set to ± 10% to increase the accuracy of the result value for performance evaluation.

Indicators for evaluation of the collimator were sensitivity, spatial resolution, and SNR. Sensitivity was calculated as the number of gamma rays absorbed by the scintillator at the rear of the collimator, and then normalization was carried out to compare the relative ratio. In the case of spatial resolution, PSF and Gaussian distribution of the profile absorbed by each pixel were analyzed, and the full-width-at-half-maximum (FWHM) and SNR were calculated using the elements shown in the formula and Fig. 3.

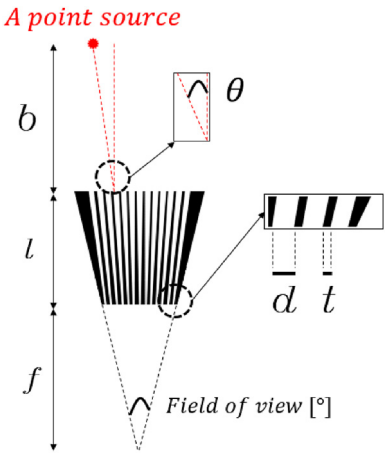

Fig. 1. Parameters for diverging collimator resolution R_{divg} and efficiency ρ for formula (X) to (Y).

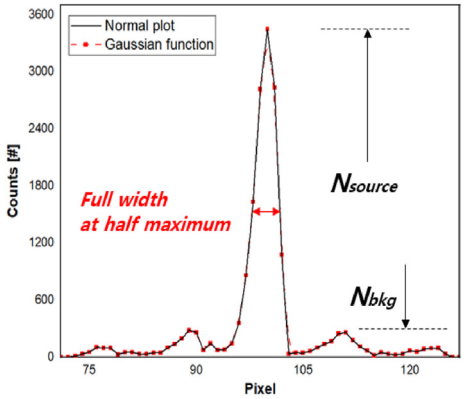

Fig. 3. Parameters of the signal-to-noise measurements in gamma images using point source.

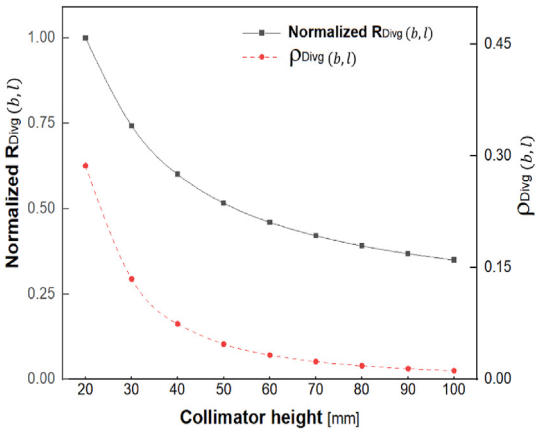

Fig. 4. Plots of normalized collimator resolution and efficiency as parameters of collimator.

$$\mathrm{FWHM} = \sqrt{2 \times \ln(2)} \times 2\sigma$$

$$\mathrm{SNR} = \frac{N_{source+bkg} - N_{bkg}}{\sqrt{N_{bkg}}}$$

Where σ is the standard deviation, N_{source} is the height of the signal at the profile peak, and N_{bkg} is the height of the background noise. In the optimization procedure using these performance indicators, the collimator height that has the greatest effect on the weight and size of the gamma camera was first shortened. Also, quickly identify the source, optimization was carried out by adjusting the hole size and the septal thickness to increase the sensitivity, as well as acquire excellent spatial resolution by reducing artifacts.

3. Results

When the point source was located at the center in FOV ($\theta = 0°$), the collimator resolution according to the collimator height became better as the height increased, as shown in Fig. 4. At a collimator height of 50.0 mm, the collimator resolution and efficiency were about 5.6% and 9.5% better than at a height of 40.0 mm, respectively. Also, the collimator resolution and efficiency were about 5.6% and 5.1% superior, respectively, compared with 50.0 mm at a collimator height of 60.0 mm. It showed a performance improvement of 4% or less at 60.0 mm or higher.

The larger is the hole size of the diverging collimator and the thinner is the septal thickness, the higher is the sensitivity of the penetration gamma rays reaching the scintillator, and the worse was the spatial resolution [14]. After initially setting the FWHM to be finally calculated as 3.0 mm, optimization was carried out, and as

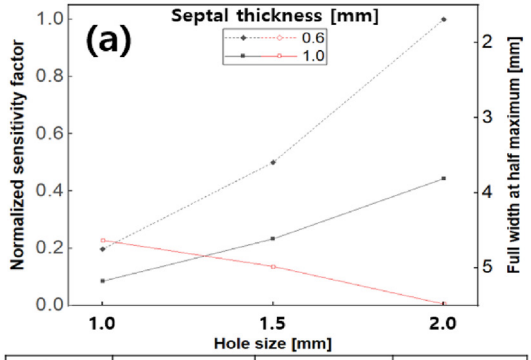

Hole size [mm]	1.0		1.5		2.0	
Septal [mm]	0.6	1.0	0.6	1.0	0.6	1.0
SNR	*14.0*	*20.7*	*14.8*	*20.8*	*15.9*	*23.7*

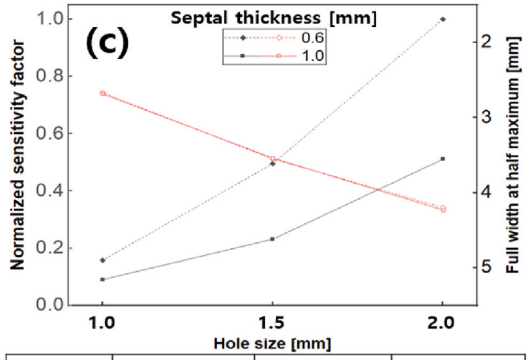

Hole size [mm]	1.0		1.5		2.0	
Septal [mm]	0.6	1.0	0.6	1.0	0.6	1.0
SNR	*53.5*	*98.0*	*38.4*	*72.0*	*35.8*	*57.1*

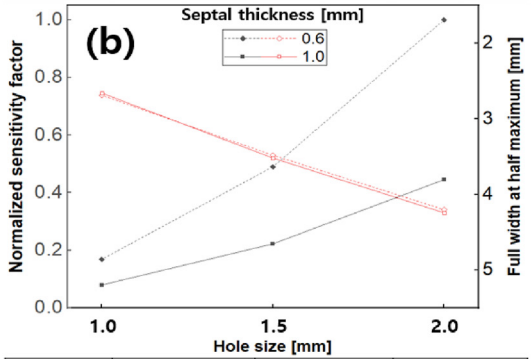

Hole size [mm]	1.0		1.5		2.0	
Septal [mm]	0.6	1.0	0.6	1.0	0.6	1.0
SNR	*40.6*	*73.9*	*32.5*	*53.5*	*29.1*	*47.1*

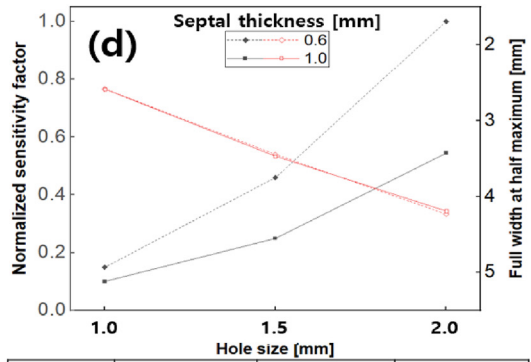

Hole size [mm]	1.0		1.5		2.0	
Septal [mm]	0.6	1.0	0.6	1.0	0.6	1.0
SNR	*72.7*	*149.8*	*49.0*	*95.5*	*41.8*	*69.5*

Fig. 5. Trade-off plots and tables as a functions of hole size with various septal thickness at (a) 50.0 mm (b) 60.0 mm (c) 70.0 mm (d) 80.0 mm of collimator height.

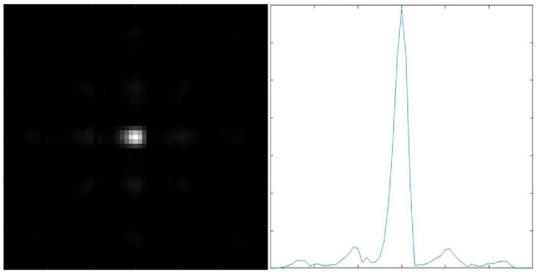

Fig. 6. Gamma image and profile acquired using optimized diverging collimator and point source.

shown in Fig. 5, the hole size was fixed to 1.0, 1.5, and 2.0 mm. Meanwhile, the septal thickness was changed to 0.6 mm and 1.0 mm to evaluate the performance variation according to collimator heights of 50.0, 60.0, 70.0, and 80.0 mm.

As a result, in (a) 50.0 mm, the artifacts in the gamma images appeared due to overall penetration. The average FWHM of about 5.0 mm was shown, despite the exclusion of combinations (hole size 1.5 mm and septal thickness 1.0 mm, and hole size 2.0 mm and septal thickness 0.6 mm) in which the source position could not be detected. In SNR, all combinations show values lower than 25.0, indicating that there are many signals of background noise compared to the peak in the gamma images, which is not suitable for detecting the correct source position.

At (b) 60.0 mm, artifacts were found in all hole sizes due to penetration at a septal thickness of 0.6 mm, and the SNR was relatively low. The source could be detected at a septal thickness of 1.0 mm, but the sensitivity was very low at a hole size of 1.0 mm. However, at the hole size of 1.5 mm, the artifacts were slightly identified from the surrounding pixels, but the SNR was at an acceptable level. In the case of the hole size of 2.0 mm, the SNR was less than 50.0, and the sensitivity of the peak was low.

In (c) 70.0 mm, the tendency of reduction in sensitivity according to hole size was very similar compared to when the height was (b) 60.0 mm, and the FWHM was less than about 2% difference in all combinations. Last, at (d) 80.0 mm, similar sensitivity reduction tendencies and performance differences less than about 4% in all combinations were confirmed. The SNR at the peak was excellent because the value of the background noise was quite low.

The SNR for confirming a meaningful gamma image capable of accurately detecting the position of the point source is estimated to be 50 ± 2. We determined a collimator height of 60.0 mm, a hole size of 1.5 mm, and a septal thickness of 1.0 mm as optimum parameters for the diverging tungsten-collimator to respond to ^{137}Cs. An FWHM of 3.5 mm and an SNR of 53.5 were obtained, and the gamma image and profile are shown in Fig. 6. These parameters reduced the height by about 10.0–20.0 mm compared to other combination parameters with similar performance, which directly affected the weight and manufacturing cost.

4. Discussion

The purpose of this study is to determine the optimization parameters of the diverging collimator, one of the components of gamma cameras used for environmental radiation monitoring in several industrial fields. The target radioisotope is ^{137}Cs, emitting 662.0 keV of mono gamma energy with a relatively long half-life of 30.2 years, requiring continuous monitoring. For design and fabrication, a Monte Carlo simulation tool was used as the basic step for manufacturing a compact diverging tungsten-collimator, and performance evaluation was conducted. The parameters were determined to be 60.0 mm in collimator height, 1.5 mm in hole size, and 1.0 mm in septal thickness. At this condition, the FWHM was 3.5 mm, showing excellent spatial resolution, and the SNR was 53.5, which was sufficient to detect the location of the point source.

Although there are parameters with better spatial resolution, feasibility conditions for weight and cost in the manufacturing process were considered. In addition, due to its low sensitivity, it is judged that it will take a lot of time to acquire a gamma image to identify the location of the source. By lowering the collimator height, the weight can be reduced by up to 75.6% compared to other parameters with similar FWHM, and up to 30.5% lighter than parameters with similar SNR. Since physically complex structures can be elaborately manufactured by applying the advanced DMLS metal 3D printing technology, the experiment will be conducted after manufacturing the gamma imaging system.

5. Conclusion

We proposed a compact diverging collimator's optimization structure that can be used for environmental radiation monitoring in the NPP industry. With this, the location of the source can be quickly identified in real time with excellent spatial resolution and SNR while preventing exposure to workers. The diverging collimator is used to detect a wide range of contaminated area at 45°, to improve sensitivity compared to the conventional type of pinhole collimator, and to have the advantages of compactness and lightness.

Declaration of competing interest

The authors declare that they have no known competing financial interests or personal relationships that could have appeared to influence the work reported in this paper.

Acknowledgement

This research was supported by the National Research Foundation of Korea (NRF) grant funded by the Korea government (Ministry of Education, Science and Technology) (No. 2020R1C1C1004584).

References

[1] International atomic energy agency, PRIS homepage, http://pris.iaea.org/PRIS/home.aspx.
[2] Y.C. Lai, S. Smith, Metaheuristic minimum dose path planning for nuclear power plant decommissioning, Ann. Nucl. Energy 166 (2022), 108800.
[3] S.R. Lin, H.W. Chou, J.J. Chen, International case survey and literature review of maintenance strategy for decommissioning nuclear power plant during transition period, Int. J. Press. Vessel. Pip. 198 (2022), 104654.
[4] K. Inoue, M. Arai, M. Fujisawa, K. Saito, M. Fukushi, Detailed distribution map of absorbed dose rate in air in tokatsu area of Chiba prefecture, Japan, Constructed by car-borne survey 4 Years after the Fukushima Daiichi nuclear power plant accident, PLoS One 12 (2017).
[5] V. Mubayi, R. Youngblood, Reevaluating the current U.S. Nuclear regulatory commission's safety goals, Nucl. Technol. 207 (2021) 406–412.
[6] S.H. Jung, K. Kim, W.S. Jang, H.K. Jeong, B.J. Kwon, S.U. Kuh, S.H. You, H.J. Choi, K.B. Kim, Development of a direction-sensitive gamma-ray monitoring system using a gamma camera with a dual-sided collimator: a Monte Carlo study, Appl. Radiat. Isot. 178 (2021), 109937.
[7] D.H. Han, J.H. Won, S.J. Lee, H.J. Lee, C.H. Baek, Optimization using Monte Carlo simulations of the thickness of a variable collimator for radiation monitoring, J. Korean Phys. Soc. 78 (2021) 627–633.
[8] M.I. Ahmad, M.H. Mohd, R. Nordin, F. Mohamed, A. Abu-Samah, N.F. Abdullah, Ionizing radiation monitoring technology at the verge of internet of things, Sensors 21 (2021) 1–29.
[9] S. Widodo, A. Abimanyu, R. Apribra, Development of drone mounted aerial gamma monitoring system for environmental radionuclide surveillance in BATAN, J. Phys. Conf. Ser. 1436 (2020), 012126.
[10] S.D. Metzler, J.E. Bowsher, M.F. Smith, R.J. Jaszczak, Analytic determination of pinhole collimator sensitivity with penetration, IEEE Trans. Med. Imaging 20

(2001) 730–741.
[11] H. Il Kim, C.H. Baek, S. Jung An, S.W. Kwak, Y. Hyun Chung, Gamma camera with a two-layer diverging-slat collimator for radioisotope monitoring, Nucl. Instruments Methods Phys. Res. Sect. A Accel. Spectrometers, Detect. Assoc. Equip. 698 (2013) 90–93.
[12] H. Cha, S. Leem, K. Cho, C. Kang, S. Bae, B. Yu, J. Yeom, H. Lee, K. Lee, Simulation study on the effect of constant hole length of curved diverging collimators for radiation monitoring systems, IEEE Trans. Nucl. Sci. 68 (2021) 1135–1143.
[13] J.H. Won, D.H. Han, S.J. Lee, C.H. Baek, Development of a gamma camera with a diverging collimator using DMLS 3D printing, J. Magn. 25 (2020) 606–613.
[14] S.R. Cherry, J.A. Sorenson, M.E. Phelps, Physics in Nuclear Medicine, Elsevier, Amsterdam, The Netherlands, 2012.
[15] K. Van Audenhaege, R. Van Holen, S. Vandenberghe, C. Vanhove, S.D. Metzler, S.C. Moore, Review of SPECT collimator selection, optimization, and fabrication for clinical and preclinical imaging, Med. Phys. 42 (2015) 4796–4813.
[16] V. Bom, M. Goorden, F. Beekman, Comparison of pinhole collimator materials based on sensitivity equivalence, Phys. Med. Biol. 56 (2011) 3199–3214.
[17] Y.J. Lee, D.H. Kim, H.J. Kim, The effect of high-resolution parallel-hole collimator materials with a pixelated semiconductor SPECT system at equivalent sensitivities: Monte Carlo simulation studies, J. Korean Phys. Soc. 64 (2014) 1055–1062.
[18] M. Georgiou, S. David, Development of a SiPM based gamma-ray imager using a $Gd_3Al_2Ga_3O_{12}$:Ce (GAGG:Ce) scintillator array, in: 2013 IEEE NSS/MIC, 2013, pp. 1–3.